



Biosorption of Hexavalent Chromium Over Modified Terrestrial Moss: Experimental, Kinetic, and Isotherm Studies

Feride Ulu

Received: 22 December 2022 / Accepted: 28 August 2024

© The Author(s), under exclusive licence to Springer Nature Switzerland AG 2024

Abstract In this research, activated carbon was prepared from terrestrial moss and utilized as a low-cost adsorbent to remove hexavalent chromium [Cr(VI)] from aqueous solution. The study examined important biosorption factors including initial pH (1–3), contact time (0.5–24 h), initial Cr(VI) concentration (20–400 mg/L), and biosorbent dosage (0.05–0.4 g) to assess their impact on the efficiency of modified terrestrial moss (MAC) in eliminating Cr(VI) from water. The biosorbent capacity was evaluated using different kinetic models and isotherms. The highest removal efficiency of Cr(VI) onto MAC was ascertained as 97.8% at an initial solution pH of 1, MAC dose of 0.2 g, initial Cr(VI) concentration of 50 mg. L⁻¹, and contact time of 15 h. The FTIR analysis revealed the interactions of certain functional groups in the adsorption of chromium ions. The biosorption occurred through the anionic adsorption mechanism and followed the pseudo-second order kinetic model. The experimental data was best fitted with Freundlich isotherm. Furthermore, the thermodynamic studies suggest that the biosorption process is both spontaneous and exothermic. The positive entropy change implied the randomness at the solid–liquid interface. In light of these compelling results, the study recommends the consideration of MAC as an efficient and

practical solution for the removal of Cr (VI) from aqueous environments.

Keywords Adsorption · Biosorption · Chromium (VI) · Moss · Toxic metal

1 Introduction

Cr is a transition metal that is naturally found in all sorts of environmental components such as air, water, and soil but only in trace amounts. It exists in various oxidation states, ranging from trivalent chromium, Cr(III), to hexavalent chromium, Cr(VI). Among these states, Cr(III) and Cr(VI) are the most common. Cr(III) is less mobile, quite stable and almost non-toxic, while Cr(VI) is mobile, reactive and toxic. Cr(VI) is formed naturally through the oxidation of Cr(III) in the environment. However, anthropogenic activities such as industrial processes can lead to an excess of chromium, which accumulates in the ecosystem and food chain without converting into a harmless form. The excessive amount of Cr(VI) has toxic effects on the environment and living things, including humans (Aigbe & Osibote, 2020; Shahid et al., 2017). Cr(VI) is widely discharged from effluents of industries such as tannery, electroplating, dyes, and paper production (Carolin et al., 2017; Gujre et al., 2021). World Health Organization (WHO) has set a maximum permissible concentration for Cr (VI) as 0.05 mg/L and 0.5 mg/L in drinking

F. Ulu (✉)
Environmental Engineering Department, Gebze Technical University, Kocaeli, Turkey
e-mail: fulu@gtu.edu.tr

water and industrial wastewater, respectively (Pavesi & Moreira, 2020). There is an urgent need to create affordable and eco-friendly methods to efficiently remove and recover toxic heavy metals from industrial wastewater.

The most commonly used treatment processes for Cr(VI) removal from wastewater are chemical precipitation, ion exchange, electrocoagulation, reverse osmosis, membrane separation, electro-Fenton process and adsorption (Golbaz et al., 2014; Mohammed & Sahu, 2015; Rahmani et al., 2015; Kumar et al., 2017; Mnif et al., 2017; Gogoi et al., 2018). However, these techniques have various drawbacks including high operational cost, higher quantities of sludge generation, high reagent and energy consumption, time-consuming procedures, low selectivity (Carolin et al., 2017; Iftekhar et al., 2017). Among these processes, adsorption is often preferred due to its high removal efficiency, cost-effectiveness, and easy handling (Kumar et al., 2017; Carolin et al., 2017).

The commercial activated carbon is one of the most used adsorbents for removal of the heavy metals. However, it has high cost and regeneration difficulties (Panda et al., 2017). As a result, researchers are turning their attention to producing activated carbon from natural biomass. This approach is environmentally friendly, cost-effective, and easy to perform (Afroze & Sen, 2018; Meitei & Prasad, 2013; Naghipour et al., 2020). The biosorption of heavy metals is a type of application of the sorption process. This process involves the use of certain biomolecules in biomass to bind and concentrate both cationic and anionic species of different toxic heavy metals in aqueous solutions. The biosorption process is driven primarily by the strong affinity between the multiple functional groups of the biosorbent, including hydroxyl, carboxylic acid, amide, carbonyl, and ether, and the adsorbates (Nouha et al., 2016).

In literature, various types of biomass have been investigated for industrial application such as algae, plants and their nuts, rice husk, orange peel, fish scale, and, moss etc. (Batoool et al., 2019; Bonyadi et al., 2022; Pradhan et al., 2019; Teshale et al., 2020; Xiong et al., 2023; Yusuff, 2019). Moss species, however, have been less studied compare to others. Mosses are green plants similar to algae, but they have a more complex structure resembling stems and leaves. Terrestrial mosses, also known as Bryophyta, are found in most terrestrial habitats.

They are the second largest group of land plants and are extremely rich in a variety of biologically active compounds such as phenols, protein, lipid, lignin and other aromatic compounds. These aromatic compounds consist of one or many aromatic rings with hydroxyl groups in combination of C-O groups. (Hao et al., 2015; Klaviða & Sprìòie, 2016).

The existing constraints on the application of most biosorbents, as documented in literature, are primarily attributed to their low biosorption capacities. Clearly, further investigation is needed to identify an effective biosorption process for Cr (VI) ion removal.

The primary objective of this study is to explore the use of modified terrestrial moss (MAC) as a cost-effective biosorbent for removing Cr (VI) metal ions from aqueous solutions. The study investigates the impact of key process parameters such as pH, contact time, Cr (VI) concentration, and biosorbent dosage on the efficiency of biosorption. The biosorbent undergoes comprehensive characterization using SEM, XRD, and FTIR to gain a thorough understanding of its physical, chemical, and surface morphological properties. Additionally, the study includes the examination of adsorption isotherm, adsorption kinetic, and thermodynamic studies to elucidate the interactive behaviour of Cr (VI) ions and the biosorbent surface under optimized experimental conditions.

2 Material and Methods

2.1 Chemicals

Chemicals, such as $K_2Cr_2O_7$ (Merck), H_2SO_4 (CDH) and 1,5-diphenylcarbazine (Sigma-Aldrich), were used in the biosorption experiments. pH adjustments were made by adding either HCl (1N) or NaOH (1N) to achieve the desired values. All chemicals used in the experiments were of analytical grade.

2.2 Preparation of Biosorbent

Samples of terrestrial moss were collected from a geothermal hot springs area in Yalova, Turkey, which is far away from any source of pollution. Initially, the collected mosses were rinsed several times with Milli-Q water to remove primary impurities. Following this, the whole mosses, without grinding or

disaggregation, were immersed in boiling 1 N HCl solution for 60 min to modify the sorbent surface completely. Subsequently, the mosses were washed with distilled water to eliminate excess HCl from the surface. Finally, the washed mosses were dried for 48 h in an oven at 80° C until completely dehydrated, and then powdered using a mortar. The prepared mosses, referred to as MAC, were stored in desiccator at room temperature for further adsorption experiments.

2.3 Adsorption Characterization

Fourier transform infrared (FTIR) spectroscopy study was carried out using Perkin Elmer Spectrum model in the range of 500–4000 cm^{-1} to analyze the functional groups of the samples.

A scanning electron microscope (SEM) operating at 15 kV was used, specifically a Hitachi S-4800, to study the adsorbent morphology. The X-ray diffraction (XRD) of the biosorbent was performed using Philips X'Pert X ray diffractometer (model PW 1730) with Cu K α radiation within 2 θ range of 10–80°.

2.4 Batch Adsorption Experiments

A chromium sample was prepared by dissolving a known quantity of potassium dichromate ($\text{K}_2\text{Cr}_2\text{O}_7$) in double-distilled water and used as a stock solution. Different initial solutions with varying concentrations of Cr(VI) were then prepared by diluting from the stock 1000 mg/L Cr(VI) standards. Batch adsorption tests were carried out to investigate the effects of solution initial pH (1–3), Cr (VI) concentration ($C_i = 20\text{--}400$ mg/L), and the adsorbent amount (0.05–0.4 g) on Cr(VI) adsorption. Samples of MAC were added to 200 ml glass beakers containing 50 ml of the specified Cr (VI) solution as stated by the experimental condition. The stirring speed was set at 300 rpm using a laboratory hotplate magnetic stirrer. The thermodynamic study was conducted at temperature ranging from 25° C to 45° C. After the biosorption process, the solution was filtered through filter paper, and then the residual Cr (VI) content in the filtrate was analyzed using the 1, 5-diphenylcarbazide method with a “VWR UV-1600PC spectrophotometer set to 540 nm.

The percentage removal of Cr (VI) (Re %) and adsorption capacity at equilibrium time (q_e mg/g), were calculated by the Eq. 1 and 2:

$$\text{Re}\% = (C_i - C_f)/C_i \times 100 \quad (1)$$

$$q_e = \frac{(C_i - C_e)V}{m} \quad (2)$$

where C_i and C_f are the initial and final Cr (VI) ion concentrations (mg/L), respectively, C_e is the equilibrium time concentrations of Cr (VI) (mg/L), m is the adsorbent mass (g), and V is the volume of the solution (L).

Biosorption capacity at time t as follows:

$$q_t = \frac{V(C_i - C_t)}{m} \quad (3)$$

where C_t is the concentration at any time t .

2.5 Adsorption Kinetics

In this study, pseudo first-order, pseudo second-order, and intra-particle diffusion models were applied to analyze the adsorption process. Pseudo first-order nonlinear equation (Lagergren, 1898) is expressed by Eq. (4) as,

$$\frac{dq_t}{dt} = k_1(q_e - q_t) \quad (4)$$

The equation can be rearranged into Eq. (5):

$$\log(q_e - q_t) = \log q_e - \frac{k_1}{2.303}t \quad (5)$$

where q_t is the sorption capacity (mg/g) at any time t (min) and k_1 (mg/g.min) is the rate constant of pseudo first order.

Pseudo second-order nonlinear equation (Blanchard, 1984) is presented in Eq. (6):

$$\frac{dq_t}{dt} = k_2(q_e - q_t)^2 \quad (6)$$

The Eq. (6) has been rearranged to obtain a linear form of Eq. (7):

$$\frac{t}{q_t} = \frac{1}{k_2 q_e^2} + \frac{1}{q_e}t \quad (7)$$

where k_2 ($\text{g mg}^{-1} \text{min}^{-1}$) is the rate constant of pseudo second order model.

The linearized transformation of the intra-particle diffusion model (Weber & Morris, 1963) is presented as follows:

$$q_t = k_p t^{1/2} + C \quad (8)$$

k_p intra-particle diffusion rate constant ($\text{mg g}^{-1} \text{min}^{-0.5}$) and C (mg/g) is a constant associated with the thickness of the boundary layer, where a higher value of C corresponds to a greater effect on the limiting boundary layer.

2.6 Equilibrium adsorption isotherm

In this study, the applicability of two-parameter isotherm models as Langmuir and Freundlich were tested to choose the best model for describing and predicting the adsorption of Cr(VI) onto MAC.

2.6.1 Langmuir Isotherm

The Langmuir isotherm assumes that the adsorbate molecules form a monolayer on adsorbents with homogeneous surface. The non-linear equation of the Langmuir isotherm has the general form (Nourmoradi et al., 2016),

$$q_e = \frac{Q_{max}^0 K_L C_e}{1 + K_L C_e} \quad (9)$$

$$\frac{1}{q_e} = \frac{1}{K_L * Q_{max}} \left(\frac{1}{C_e} \right) + \frac{1}{Q_{max}} \quad (10)$$

where Q_{max} (mg/g) is the maximum saturated monolayer adsorption capacity of an adsorbent, C_e (mg/L) is the adsorbate concentration at equilibrium, q_e (mg/g) is the amount of adsorbate uptake at equilibrium, and K_L (L/mg) is the Langmuir equilibrium constant related to the affinity between an adsorbent and adsorbate.

An essential factor of the Langmuir isotherm is the separation factor (R_L) which is defined as follows (Martins et al., 2015):

$$R_L = \frac{1}{1 + K_L C_o} \quad (11)$$

2.6.2 Freundlich Isotherm

The non-linear equation of Freundlich isotherm is applied for multi-layer, heterogeneous adsorption sites and is expressed as follows (does not describe the saturation behavior of an adsorbent) (Martins et al., 2015):

$$q_e = K_F C_e^{\frac{1}{n}} \quad (12)$$

$$\log q_e = \frac{1}{n} \log C_e + \log K_F \quad (13)$$

where q_e (mg/g) is the amount of adsorbate uptake at equilibrium, C_e (mg/L) is the adsorbate concentration at equilibrium, K_F ($\text{mg/g}/(\text{mg/L})^n$) is the Freundlich constant, and n (dimensionless) is the Freundlich intensity parameter, which indicates the magnitude of the adsorption driving force or the surface heterogeneity.

According to the Freundlich theory, the adsorption isotherm becomes linear when $n=1$, favorable when $n > 1$, and unfavorable when $n < 1$.

2.7 Thermodynamic Study

The temperature dependence in the biosorptive removal of heavy metal ions from aqueous solutions is associated with thermodynamic parameters as Gibbs free energy (ΔG°), enthalpy (ΔH°), and entropy (ΔS°). These thermodynamic parameters can be calculated according to the following equations:

The relationship among ΔG , ΔH , ΔS , and absolute temperature (T) is shown in Eq. (14) (Bermúdez et al., 2012).

$$\Delta G = \Delta H - T\Delta S \quad (14)$$

The ΔG values at different temperature can be computed using the law of thermodynamics as given in Eq. (15) (Pradhan et al., 2019).

$$\Delta G = -RT \ln(K_c) \quad (15)$$

where K_c is the dimensionless equilibrium constant and R is the universal gas constant. Since the Langmuir constant K_L was derived in the previous section,

the dimensionless value of K_c can be computed by the formulae given in Eq. (16) (Pradhan et al., 2019).

$$K_c = 51996 \times 55.5 \times K_L \quad (16)$$

The value 51.996 is the atomic weight of Cr in $\text{mg}\cdot\text{mol}^{-1}$. The value 55.5 is the concentration of water $\text{mol}\cdot\text{L}^{-1}$. The ΔG values at different temperature were calculated using the formulae in Eq. (15). The ΔH and ΔS were calculated according to Eq. (14). A graph of ΔG plotted versus T gives a straight line, and the slope and intercept are respectively $-\Delta S$ and ΔH .

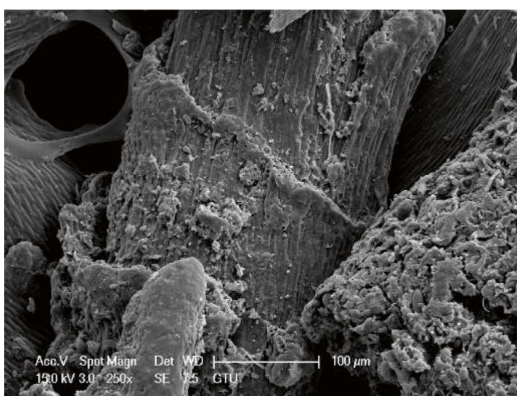
3 Results and Discussion

3.1 SEM, XRD, and FTIR Analysis of Biosorbent

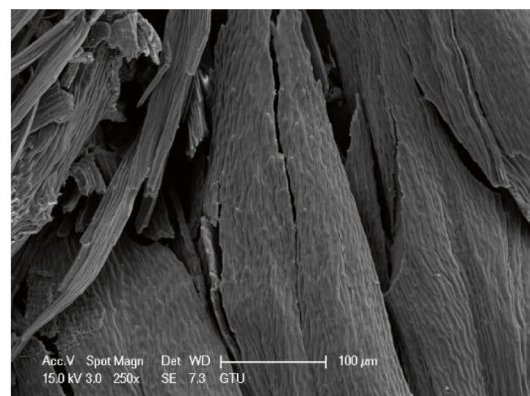
The SEM analysis of the MAC samples was conducted before and after the adsorption of Cr(VI) under optimal operating conditions with 100X magnification (Fig. 1). In Fig. 1b, it can be observed that after the loading of Cr(VI), the pores on the fresh biosorbent were covered, resulting in a relatively smooth surface due to the adsorption of Cr(VI). The X-ray diffraction (XRD) plot of MAC is shown in Fig. 2. The presence of the pointed peaks in XRD pattern indicates the crystalline nature of MAC. The characteristic diffraction peaks at $2\theta = 16.516^\circ$, 22.589° , 26.651° , and 34.898° illustrate the carbon graphitic structure of MAC

(Girgis et al., 2007). These peaks could be indexed to activated carbon (JCPDS reference No. 82–1691). Typically, a noticeable hump in the range $20\text{--}30^\circ$ represents a significant degree of disorder, which is typical of carbon structure (Adeyikna et al., 2019). The XRD plot of Cr(VI) loaded MAC indicated that the structure of biosorbent remained almost unaltered after biosorption. The XRD analysis was also confirmed by SEM analysis of both the unloaded and Cr(VI) loaded biosorbent, which revealed a change in surface roughness while maintaining the same surface morphology with less porosity.

The Fourier Transform Infrared (FTIR) spectrum analysis was conducted to comprehensively understand how functional groups on the surface of the MAC interact with Cr(VI) ions. Figure 3 illustrates the FTIR spectra of the MAC before and after the adsorption of Cr(VI). It is clear that certain peaks shifted, disappeared, and new ones emerged after the Cr(VI) biosorption, indicating a significant transformation. The broad peak at approximately 3309.4 cm^{-1} represents the typical O–H stretching vibration of hydroxyl groups. However, when the material is loaded with Cr(VI), this peak shifts to 3303.1 cm^{-1} , indicating binding of Cr(VI) with the OH group (Srivastava et al., 2016). Additionally, a new peak at 3011 cm^{-1} appears due to the coordination of Cr(VI) ions with a functional group. Furthermore, the shift in the peak from 2914.8 cm^{-1} to 2918.5 cm^{-1} , confirming Cr(VI) binding with



a)



b)

Fig. 1 SEM images of (a) fresh MAC and (b) Cr(VI) ions loaded MAC

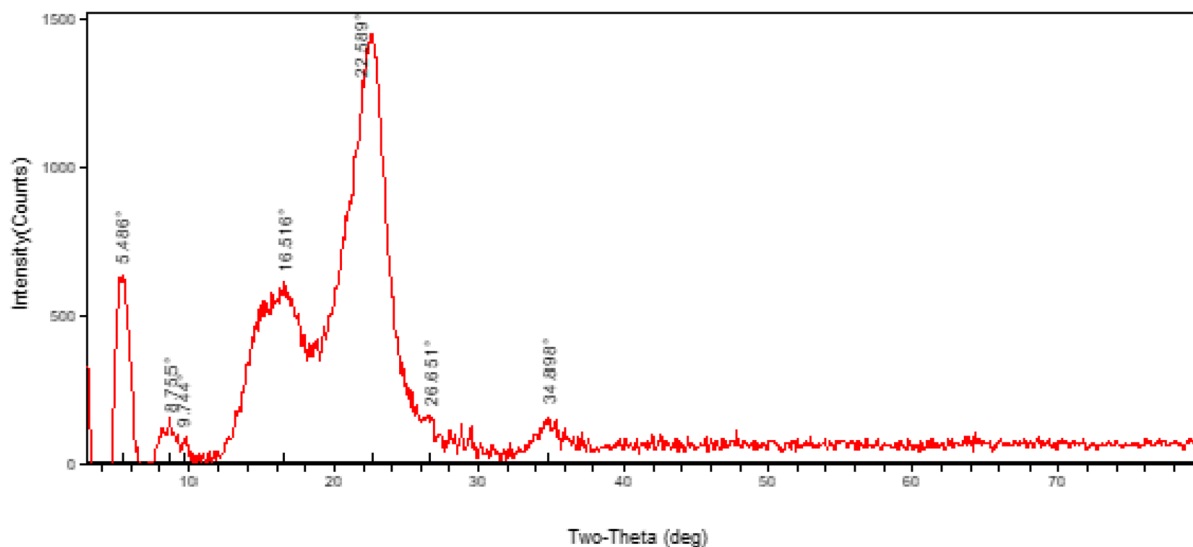
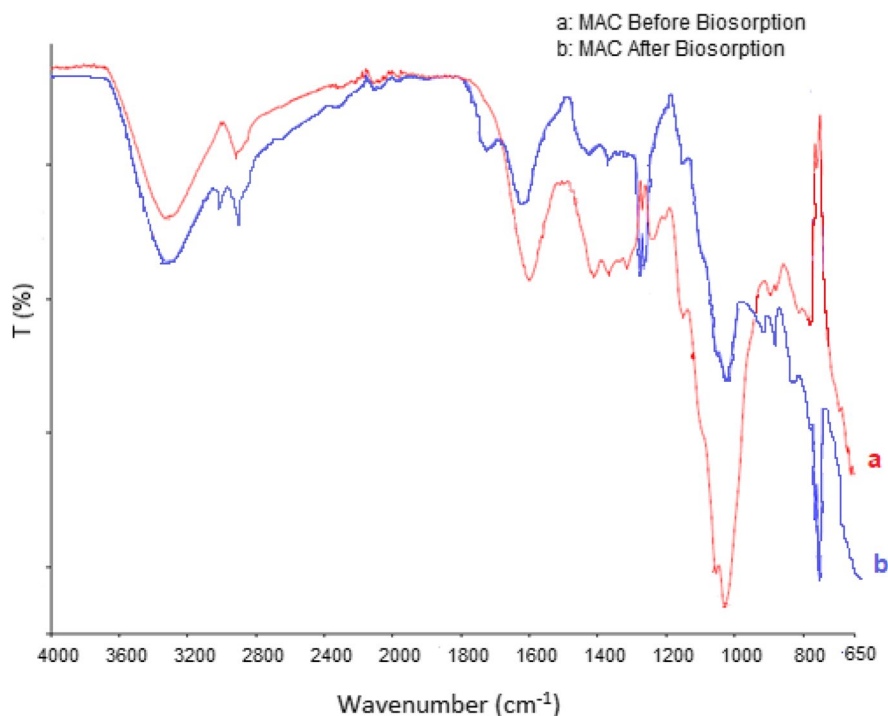


Fig. 2 XRD diffraction patterns of fresh MAC

Fig. 3 FTIR spectra of **a)** before and **b)** after Cr (VI) biosorption



aliphatic C-H groups. The band observed at about $1599,6\text{ cm}^{-1}$ could be assigned to the stretching band of the free carbonyl double bond ($\text{C}=\text{O}$) from the carboxyl functional group that may be attributed to lignin aromatic group. The peak at $1410,8\text{ cm}^{-1}$ could correspond to the bending vibration of $-\text{NH}$ group.

The biosorption bands at $1240,9\text{ cm}^{-1}$ and 1150 cm^{-1} and $1058,1\text{ cm}^{-1}$ could be assigned to C-O stretching in the carboxylic acid and $-\text{C}-\text{C}$ -group, respectively.

Furthermore, the absence of a peak suggests that residual carboxylate groups have been transformed into carboxylic acid groups, as expected at such a low

pH (Solisio et al., 2013). Therefore, the changes in the FTIR pattern indicate the successful chemical modification of terrestrial moss into MAC and the interaction of Cr(VI) with acidic carboxyl (C-O and C=O), hydroxyl (O-H), and amine (N-H) groups present on the MAC surface.

3.2 Effect of Initial pH and Contact Time

The pH of the aqueous solution is an essential factor affecting biosorption of toxic heavy metal onto biosorbent. This dependency is both related to the surface properties of the biosorbent and chromium species in solution. The occurrence of active side on biosorbent depends on protonation reactions between functional groups of biosorbent and ambient. The ionization of functional groups leads to the formation of negative or positive charges (such as -COO^- or -COOH_2^+) on biosorbent surface. Through electrostatic attraction, positively or negatively charged heavy metals can be fixed on the biosorbent (Qiu et al., 2021).

The distribution of Cr (VI) species is primarily influenced by pH and adsorbent properties. Between pH 1 and 4, the dominant oxyanion form of Cr (VI) is HCrO_4^- . As the solution pH increases, the concentration of HCrO_4^- shifts to other forms, CrO_4^{2-} and $\text{Cr}_2\text{O}_7^{2-}$. Above pH 6, CrO_4^{2-} becomes dominant, while $\text{Cr}_2\text{O}_7^{2-}$ is the predominant Cr(VI) species at acidic pH (Gottipati & Mishra, 2016).

The data in Fig. 4 clearly showed that the removal of Cr(VI) from the solution occurs much more rapidly at pH 1 and 1.5 compared to at pH 2, 2.5, and 3. This is likely due to the affinity between the adsorbent and Cr species, resulting in a swift initial adsorption rate at pH 1 and 1.5. Chen et al. found that Cr species have different affinities to be adsorbed and reduced (Chen et al., 2011). Initially, adsorption takes place rapidly due to the abundance of available active sites.

As seen in Fig. 4a it was found that approximately 80% of Cr(VI) adsorption onto MAC occurred within 3 h, and this adsorption process reached equilibrium in 6 h at pH 1. At this pH, after the optimum removal efficiency reached 97.82% in 15 h, the desorption was observed. Furthermore, the removal efficiency of Cr (VI) was 59% in 3 h, and maximum removed Cr (VI) was 91.42% at pH 1.5. Equilibrium was consistently achieved at approximately 15 h, after which the removal efficiency gradually decreased until 25 h. The removal efficiency followed the order of pH $2 > \text{pH } 2.5 > \text{pH } 3$, with values of 80%, 45%, and 38%, respectively, at 15 h, and then decreased further.

In the biosorption study, after the active binding site of the respective functional groups was saturated, the biosorption reached equilibrium. Also, the inner pores of the biosorbent could become full for adsorption of Cr (VI) as seen in Fig. 1.

The adsorption density and removal efficiency of Cr (VI) gradually decreased after 15 h of processing time at all initial pH levels. This suggests that the

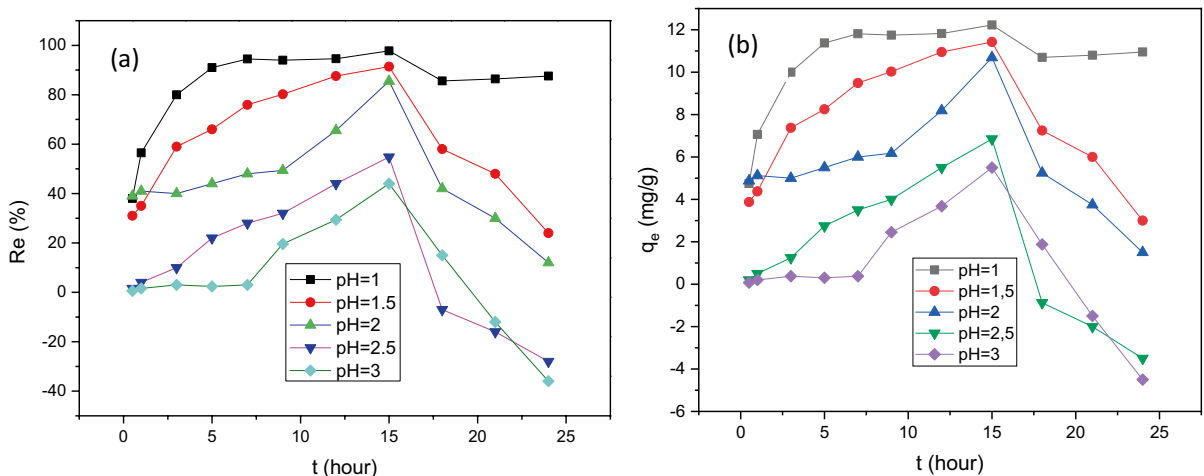
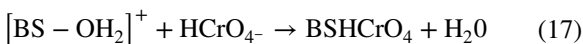


Fig. 4 Effect of initial pH on **a**) Cr (VI) removal efficiency by MAC **b**) adsorption capacity ($C_i = 50 \text{ mg.L}^{-1}$)

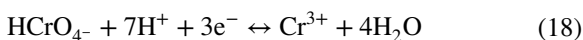
desorption of the Cr (VI) molecule occurred from the biosorbent surface. This could be attributed to the physisorption nature of adsorption, where the chromium molecule tends to revert after reaching equilibrium or when the biosorbent site becomes saturated (Halder et al., 2016; Sharma et al., 2013).

Figure 4b clearly demonstrates that the maximum adsorption capacity occurred at pH 1, reaching 11.9 mg/g. This capacity gradually decreased as the initial pH values increased. At the highest pH of 3, the adsorption capacity dropped to 5.5 mg/g. It was observed that the adsorption of chromium anions on the biosorbent surface decreased with increasing pH value. At low pH values, the surface of MAC was positively charged. Therefore, the study suggested that the predominant species was the HCrO_4^- adsorbed onto protonated (positively charged) sites of the biosorbent's surface at strong acidic pH levels, in accordance with Eq. 17. These findings are consistent with those of previous studies (Doke & Khan, 2017; Panda et al., 2017). Based on these observations, the adsorption mechanism is likely physical biosorption due to electrostatic interaction between the positively charged sites and negatively charged species under acidic conditions.



where $[\text{BS} - \text{OH}_2]^+$ is one of the representative protonated active functional group on biosorbent surface of prepared active carbon.

As the initial pH of the solution was increased, the functional groups on the surface of the biosorbent became less protonated, resulting in an increase in negative charge on the surface. This led to a reduction in the affinity of Cr(VI) anions to the biochar. The higher concentration of OH^- ions also hindered the diffusion of Cr(VI) complexes to the surface. Conversely, under acidic conditions, Cr(VI) complexes could have been further reduced by electrons provided by MAC, as mentioned in the work of Gogoi et al., 2018 and Usman et al., 2015 (Eq. 18).



Under strongly acidic conditions, the presence of positively charged H^+ ions on the surface of the MAC can lead to electrostatic repulsion between Cr(III) ions and the bioadsorbent. As the pH increases, the MAC surface becomes negatively charged, facilitating electrostatic

attraction between the MAC and Cr(III) ions. However, in this study, at the examined pH values (1–3.5), Cr(III) precipitates as $\text{Cr}(\text{OH})_3$. Therefore, the precipitation of Cr(III) and/or other mechanisms for Cr(III) removal can be excluded based on the research in the literature (Gogoi et al., 2018; Zouboulis et al., 1995).

At pH 1 and 1.5, the contact time was sufficient to achieve real equilibration of adsorbent and adsorbate. Therefore, using data taken a significant time after reaching equilibrium or very close to equilibrium could lead to erroneous conclusions regarding adsorption kinetics. For this reason, the optimum contact time was set at 7 h and the initial pHs were set at 1, 1.5 and 2 for the further experiments.

3.3 Effect of Initial Cr (VI) Concentration and Biosorbent Dosage

A large amount of chromium (VI) was adsorbed when lower concentrations were used as seen in Fig. 5. With a change in the initial concentration of the Cr(VI) solution from 20 to 400 mg/L, the removal efficiency of Cr(VI) decreased from 98.5% to 62% at pH 1, from 96.7% to 48% at pH 1.5 and from 82.5% to 43% at pH 2, respectively. At low concentrations, the available surface area of the adsorbent was large. As a result, fractional adsorption became independent of the initial concentration. However, at higher concentrations, available adsorption sites became fewer and Cr(VI) removal percentage decreased (Deveci & Kar, 2013; Panda et al., 2017).

It was also observed (the graph was not given) that the adsorption density of Cr(VI) on the MAC increased with increasing initial concentration. As the Cr(VI) concentration increased from 20 mg/L to 400 $\text{mg}\cdot\text{L}^{-1}$ at pH 1, the adsorption capacity increased from 4.93 $\text{mg}\cdot\text{g}^{-1}$ to 62.03 $\text{mg}\cdot\text{g}^{-1}$. Deveci and Kar reported that the values of q_e , for the adsorbents studied, were greater at higher initial concentration, explaining that the initial concentration was a key driving force to overcome the mass transfer resistance of Cr(VI) ions between the liquid and solid phases (Deveci & Kar, 2013).

The amount of biosorbent added is another factor that has an influence on the performance of the biosorption process. As shown in Fig. 6, it had a positive correlation with the Cr(VI) adsorbed on the surface at an optimum contact time of 7 h and at pH 1.5. The removal efficiency of Cr(VI) reached more

Fig. 5 The effect of initial Cr(VI) concentration on Cr(VI) removal by MAC at different initial pHs (contact time 7 h, adsorbent dosage 0.2 g)

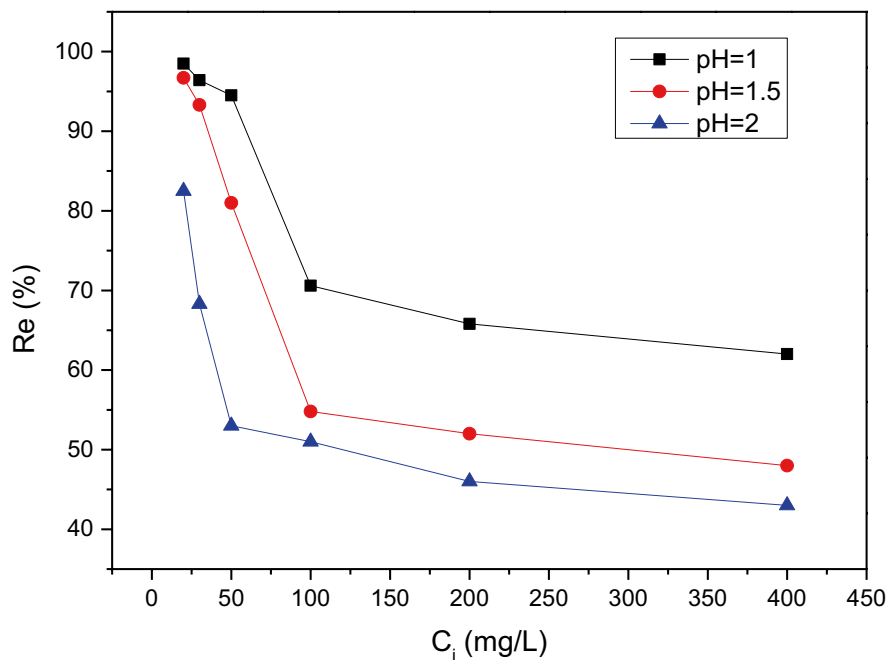
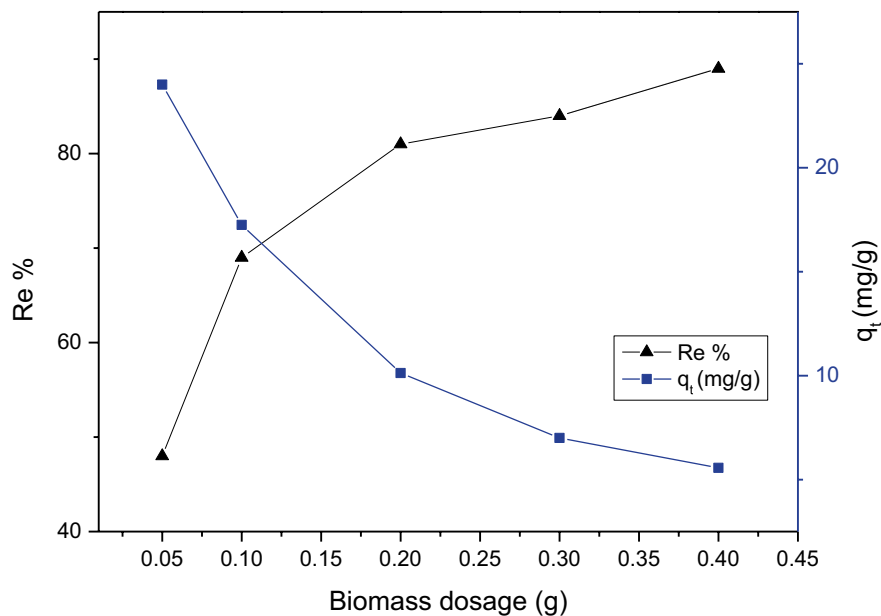


Fig. 6 The effect of biomass dosage on Cr(VI) removal efficiency and q_t



than 80% when the dosage of MAC was 0.2 g/50 ml. However, while the adsorption capacity of MAC decreased from 11 to 4 $\text{mg}\cdot\text{g}^{-1}$, the removal efficiency of Cr(VI) did not change much when the concentration was further increased to 0.4 g/mL. An increase in the dosage of the biosorbent led to a decrease in the biosorption

capacity as $25 \text{ mg}\cdot\text{g}^{-1}$ was observed at lowest MAC loading of 0.05 g/50 ml. This inverse relationship may be due to the formation of agglomerated biosorbent particles at high biomass loading, with the net effect of reducing the available metal binding site. A similar observation has been reported in recent investigations (Naseem et al., 2019; Ume et al., 2022).

3.4 Kinetics Studies (Fig. 7)

In the study, the applicability of three different kinetic models as pseudo first order, pseudo second order and intraparticle diffusion were tested to investigate the adsorption rate of Cr(VI) on MAC at initial pH 1, 1.5 and 2. The intra-particle diffusion model was fitted to the kinetic data in order to understand the diffusion mechanism and the rate-controlling step in the adsorption process.

The kinetic parameters of the pseudo-first-order and pseudo-second order models were evaluated from the combined plots of $\log (q_e - q_t)$ versus t and t/q_t against t using Eq. 5 and Eq. 7, respectively, while the parameters contained in the intra-particle diffusion model were obtained from the plot of q_t versus $t^{1/2}$ according to Eq. 8 (Fig. 8). Table 1 shows the calculated kinetic constants and R^2 coefficients for each kinetic model. The pseudo-second-order kinetic model had an R^2 value closer to 1 (0.9982) than the value of 0.9067 obtained for the pseudo-first-order model. This means that, as seen in Fig. 7, the pseudo-second-order kinetic model was the best fitting model for all the pH values studied. The obtained experimental data for q_e (mg.

g^{-1}) as 12.52, 11.54 and 10.84 were favourably predicted by the pseudo-second-order model as shown in Table 1 at pH 1, 1.5 and 2, respectively. Similar results have been reported by several researchers (Prabhu et al., 2020; Pant et al., 2022).

The value of R^2 for the intra-particle diffusion model given in Table 1 did not confirm that the kinetic model was actually the rate-determining step. However, it was evidently clear that intra-particle diffusion participated in the rate-limiting step. As seen in Fig. 6, the plot of q_t versus $t^{1/2}$ did not pass through the origin. Thus, the intra-particle diffusion could not be regarded as the only rate-limiting step in the biosorption process (Yusuff, 2019). The fitted model showed a multi-stages adsorption process (Fig. 8). The first step is the dispersion through the solution to the external surface of the biosorbent or the boundary layer diffusion of the solute molecules. The second step corresponds to the intraparticle or pore diffusion, in which Cr(VI) ions are diffused from the surface into the biosorbents' pores. The third linear stage indicates interaction between target adsorbate and active sites and the equilibrium phase (Norouzi et al., 2018; Zheng et al., 2018).

Fig. 7 Pseudo-second-order kinetics for biosorption of Cr(VI) on MAC ($Cr(VI)_i = 50$ mg/L, adsorbent mass = 0.2 g, $V = 50$ mL, and contact time = 7 h at $25^\circ C$)

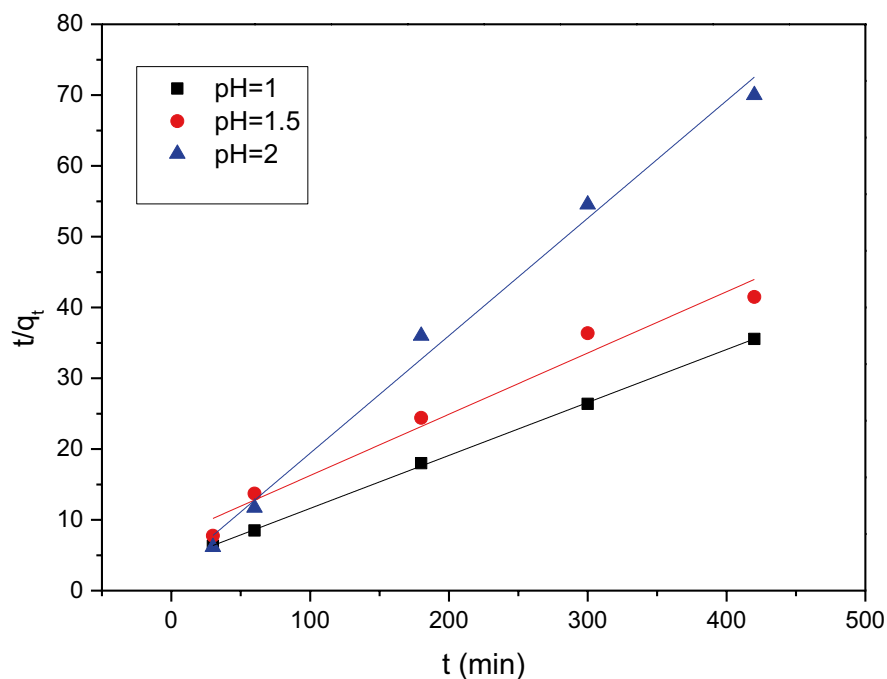


Fig. 8 The intraparticle diffusion kinetic model for the removal of Cr(VI) ($C_i = 50$ mg/L, adsorbent mass = 0.2 g, $V = 50$ mL, and contact time = 7 h at 25 °C)

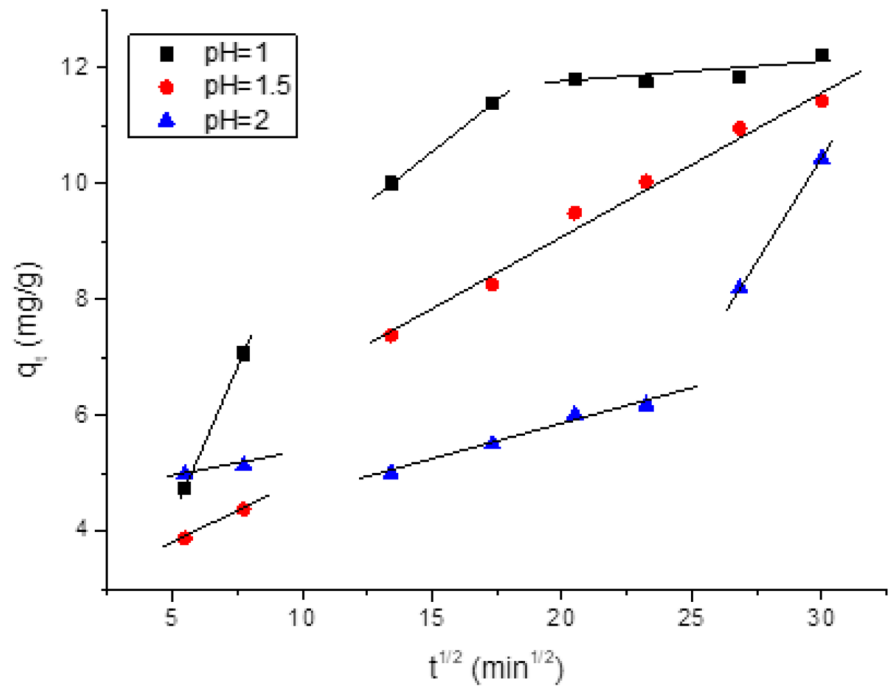


Table 1 Kinetic model parameters for the removal of Cr (VI) ($C_i = 50$ mg/L, adsorbent mass = 0.2 g, $V = 50$ mL, and contact time = 7 h at 25 °C)

Kinetic model	Parameters	Initial pH		
		1	1.5	2
Pseudo first order	k_1 (min^{-1})	6.129E-3	4.145E-3	4.606E-4
	q_e , cal (mg/g)	8.224	9.084	6.074
	R^2	0.9862	0.9625	0.8559
Pseudo second order	k_2 (g/mg/min)	0.00135	9.875E-4	9.779E-3
	q_e , cal (mg/g)	13.369	11.547	6.024
	R^2	0.9996	0.973	0.9916
Intra-particle diffusion	K_p (mg/g $\text{min}^{1/2}$)	0.464	0.416	0.063
	C	3.013	1.440	4.482
	R^2	0.9438	0.9852	0.7714

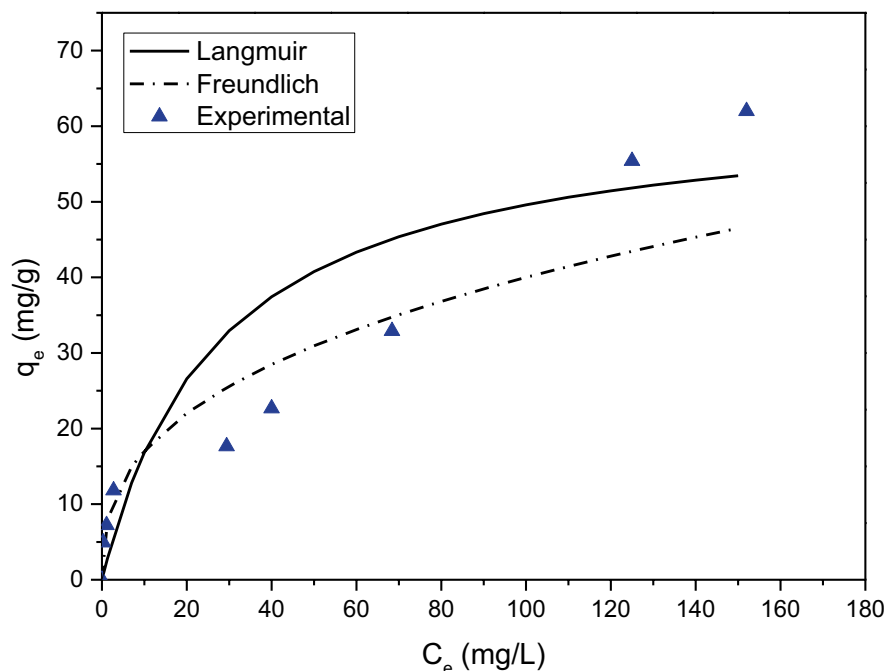
3.5 Adsorption Equilibrium Modeling

Adsorption isotherms are used to gain an understanding of how the adsorbate molecules are partitioned between the aqueous phase and the solid phase under conditions of equilibrium (Martins et al., 2015). In order to test the applicability of Langmuir and Freundlich, the initial concentration of Cr(VI) was used in the range of 20 to 400 mg/L. Plots of $1/q_e$ vs. $1/C_e$ (Langmuir plot) and $\ln q_e$ vs. $\ln C_e$ (Freundlich plot) [figures not shown] were drawn according to Eqs. 10 and 13 at three different initial pHs of 1, 1.5 and 2. The obtained Langmuir and Freundlich adsorption

constants and regression correlation coefficients were given in Table 1.

The experimental data, Langmuir, and Freundlich isotherms were plotted as q_e versus C_e using non-linear Eqs. (2), (9) and (12) respectively. A comparison of the experimental data with the Langmuir and Freundlich isotherms was shown in Fig. 9. The linear correlation coefficient (R^2) was used to assess the applicability of the isotherms. Based on the R^2 values, the Freundlich isotherm best fitted the Cr(VI) adsorption equilibrium data with 0.9482, 0.9227 and 0.9551 at pH 1, 1.5 and 2 respectively. This indicated that the adsorption of Cr(VI) by the MAC adsorbent was

Fig. 9 Adsorption isotherm of Cr(VI) onto MAC and non-linear adjustments of the isotherm models ($C_i=20\text{--}400\text{ mg/L}$, $T=25^\circ\text{C}$, $t=420\text{ min}$)



apparently carried out with multi-layered and heterogeneous adsorption sites. A similar observation was reported for the adsorption of Cr(VI) from an aqueous solution by other natural biosorbents in the literature (Ume et al., 2022; Yusuff, 2019). The magnitude of the Freundlich exponent ($n=2.699$) indicated that adsorption of Cr(VI) on MAC was favorable (Saleh et al., 2017).

An essential factor of the Langmuir isotherm is the separation factor (RL), which can be used to verify whether the adsorption process is favourable ($0 < RL < 1$), linear ($RL = 1$) or unfavourable ($RL > 1$) (Martins et al., 2015). For the range of applied concentration (20–400 mg/L), the RL values decreased from 0.580 to 0.0646 at pH 1 and from 0.6993 to 0.1042 at pH 1.5 and from 0.9995 to 0.9058 at pH 2. The obtained Langmuir and Freundlich adsorption constants and regression correlation coefficients were given in (Table 2).

3.6 Thermodynamic Studies

The thermodynamic parameters were determined in order to elucidate the inherent energy changes involved in the biosorption process and to ascertain the mechanism of biosorption. The effect of temperature on the uptake of Cr(VI) on MAC was investigated

Table 2 Isotherm model parameters for the removal of Cr(VI) ($C_i=50\text{ mg/L}$, adsorbent mass = 0.2 g, $V=50\text{ mL}$, and contact time = 7 h at 25°C)

Isotherm models	Parameters	Initial pH		
		1	1.5	2
Langmuir	Q_{\max} (mg/g)	63.33	50.52	62.11
	K_L (L/mg)	0.0362	0.0215	0.0073
	R^2	0.8485	0.8313	0.7503
Freundlich	K_F ((mg/g)(L/mg) ^(1/n))	7.26	5.055	0.415
	n	2.699	2.772	2.932
	R^2	0.9482	0.9227	0.9551

at 298, 308 and 318 K. The thermodynamic parameters Gibbs free energy (ΔG°), enthalpy (ΔH°) and entropy (ΔS°), which explain the spontaneity and the exothermic or endothermic nature of the biosorption process (Bermúdez et al., 2012). The thermodynamic parameters were calculated using Eqs. 11, 12 and 13 as shown in Table 3. At all temperatures, the negative values of ΔG° indicate that the adsorption process is spontaneous. The negative ΔH° denotes an exothermic biosorption process, which makes the biosorption process studied physical in nature (physisorption). An increase in temperature leads to a decrease

Table 3 Thermodynamic parameters for the adsorption of Cr(VI) onto MAC

ΔG° in $\text{kJ}\cdot\text{mol}^{-1}$			ΔH° in $\text{kJ}\cdot\text{mol}^{-1}$	ΔS° in $\text{J}\cdot\text{mol}^{-1}\cdot\text{K}^{-1}$	R^2
Temperature in K					
298	308	318			
-28.632	-28.744	-28.802	-26.095	0.0085	0.99

in adsorption (Gupta et al., 2010). A positive ΔS° means that the randomness in the solid/solution interface is increasing during the fixation of Cr (VI) on the active sites of the adsorbent.

4 Conclusion

The purpose of the present work was to investigate the efficiency of chemically modified terrestrial moss as a biosorbent for the removal of Cr(VI) ions from aqueous solutions. In order to determine the optimum conditions for the uptake of Cr(VI) on the MAC surface, the important biosorption process parameters such as initial pH, contact time, initial Cr(VI) concentration and biosorbent dosage were examined. The highest removal efficiencies of Cr(VI) by MAC were obtained under strong acidic conditions as 97.8% and 91.4% with an adsorption capacity of 12.22 and 11.42 mg/g at pH 1 and 1.5, respectively, for $C_i = 50 \text{ mg}\cdot\text{L}^{-1}$ at 15 h. Cr(VI) readily adsorbed on MAC surface at pH 1 and 1.5, resulting in higher adsorption rates. The biosorption of Cr(VI) is significantly pH dependent, and the best results can be obtained at $\text{pH} < 2$. It can be concluded that the main biosorption mechanism during the adsorption process at $\text{pH} < 3$ was the electrostatic attraction (known as outer-sphere complexation) between Cr(VI) anions and the positively charged surface of the biosorbent. FTIR spectroscopic data show that MAC is rich in heterogeneous functional groups, mainly acidic carboxyl, hydroxyl and amine groups, which interact with Cr(VI). The adsorption kinetic studies indicate that the biosorption of Cr(VI) on MAC is a pseudo-second-order kinetic model chemisorption and the intraparticle pore diffusion mechanism is involved in adsorbing Cr(VI) on MAC. The removal of Cr(VI) obeys the Freundlich model, which describes the

surface of the MAC as being heterogeneous and having multilayer adsorptive properties. The MAC could be considered as a potential adsorbent for the removal of Cr(VI) from aqueous solutions for further research in the future.

Funding No funding was received to assist with the preparation of this manuscript.

Data Availability All necessary data are included in the document.

Declarations

Ethical Approval This article does not contain any studies with human participants or animals performed by any of the authors.

Conflict of Interest The authors declare that they have no conflict of interest.

References

- Afroze, S., & Sen, T. K. (2018). A review on heavy metal ions and dye adsorption from water by agricultural solid waste adsorbents. *Water, Air, & Soil Pollution*, 229(7), 1–50.
- Aigbe, U. O., & Osibote, O. A. (2020). A review of hexavalent chromium removal from aqueous solutions by sorption technique using nanomaterials. *Journal of Environmental Chemical Engineering*, 8, 104503. <https://doi.org/10.1016/j.jece.2020.104503>
- Batool, S., Idrees, M., Al-Wabel, M.I., Ahmad, M., Hina, K., Ullah, H., ... & Hussain, Q. (2019) Sorption of Cr (III) from aqueous media via naturally functionalized microporous biochar: Mechanistic study. *Microchemical Journal*, 144:242–253. <https://doi.org/10.1016/j.microc.2018.09.012>
- Bermúdez, Y. G., Rico, I. L. R., Guibal, E., de Hoces, M. C., & Lara, M. A. M. (2012). Biosorption of hexavalent chromium from aqueous solution by *Sargassum muticum* brown alga. Application of statistical design for process optimization. *Chemical Engineering Journal*, 183, 68–76. <https://doi.org/10.1016/j.cej.2011.12.022>
- Blanchard, G., Maunay, M., & Martin, G. (1984). Removal of heavy metals from waters by means of natural zeolites. *Water Resource*, 18(12), 1501–1507. [https://doi.org/10.1016/0043-1354\(84\)90124-6](https://doi.org/10.1016/0043-1354(84)90124-6)
- Bonyadi, Z., Nasoudari, E., Ameri, M., Ghavami, V., Shams, M., & Sillanpää, M. (2022). Biosorption of malachite green dye over *Spirulina platensis* mass: Process modeling, factors optimization, kinetic, and isotherm studies. *Applied Water Science*, 12(7), 1–11. <https://doi.org/10.1007/s13201-022-01690-8>
- Carolyn, F. C., Kumar, P. S., Saravanan, A., Joshiba, G. J., & Naushad, M. (2017). Efficient techniques for the removal of toxic heavy metals from aquatic environment: A

- review. *Journal of Environmental Chemical Engineering*, 5, 2782–2799. <https://doi.org/10.1016/j.jece.2017.05.029>
- Chen, G. Q., Zhang, W. J., Zeng, G. M., Huang, J. H., Wang, L., & Shen, G. L. (2011). Surface modified phanerochaete chrysosporium as a biosorbent for Cr(VI)-contaminated wastewater. *Journal of Hazardous Material*, 186, 2138–2143. <https://doi.org/10.1016/j.jhazmat.2010.12.123>
- Deveci, H., & Kar, Y. (2013). Adsorption of hexavalent chromium from aqueous solutions by bio-chars obtained during biomass pyrolysis. *Journal of Industrial and Engineering Chemistry*, 19(1), 190–196. <https://doi.org/10.1016/j.jiec.2012.08.001>
- Doke, K. M., & Khan, E. M. (2017). Equilibrium, kinetic and diffusion mechanism of Cr (VI) adsorption onto activated carbon derived from wood apple shell. *Arabian Journal of Chemistry*, 10, S252–S260. <https://doi.org/10.1016/j.arabjc.2012.07.031>
- Girgis, B. S., Temerk, Y. M., Gadelrab, M. M., & Abdullah, I. D. (2007). X-ray diffraction patterns of activated carbons prepared under various conditions. *Carbon Letters*, 8(2), 95–100. <https://doi.org/10.5714/CL.2007.8.2.095>
- Gogoi, S., Chakraborty, S., & Saikia, M. D. (2018). Surface modified pineapple crown leaf for adsorption of Cr (VI) and Cr (III) ions from aqueous solution. *Journal of Environmental Chemical Engineering*, 6(2), 2492–2501. <https://doi.org/10.1016/j.jece.2018.03.040>
- Golbaz, S., Jafari, A. J., Rafiee, M., & Kalantary, R. R. (2014). Separate and simultaneous removal of phenol, chromium, and cyanide from aqueous solution by coagulation/ precipitation: Mechanisms and theory. *Chemical Engineering Journal*, 253, 251–257. <https://doi.org/10.1016/j.cej.2014.05.074>
- Gottipati, R., & Mishra, S. (2016). Preparation of microporous activated carbon from Aegle Marmelos fruit shell and its application in removal of chromium (VI) from aqueous phase. *Journal of Industrial and Engineering Chemistry*, 36, 355–363. <https://doi.org/10.1016/j.jiec.2016.03.005>
- Gujre, N., Mitra, S., Soni, A., Agnihotri, R., Rangan, L., Rene, E. R., & Sharma, M. P. (2021). Speciation, contamination, ecological and human health risks assessment of heavy metals in soils dumped with municipal solid wastes. *Chemosphere*, 262, 128013. <https://doi.org/10.1016/j.chemosphere.2020.128013>
- Gupta, V. K., Rastogi, A., & Nayak, A. (2010). Biosorption of nickel onto treated alga (*Oedogonium hatei*): application of isotherm and kinetic models. *Journal of colloid and interface science*, 342(2), 533–539. <https://doi.org/10.1016/j.jcis.2009.10.074>
- Halder, G., Khan, A. A., & Dhawane, S. (2016). Fluoride sorption onto a steam-activated biochar derived from *Cocos nucifera* shell. *Clean: Soil, Air, Water*, 44(2), 124–133. <https://doi.org/10.1002/clen.201400649>
- Hao, D. C., Gu, X. J., & Xiao, P. G. (2015). Chemotaxonomy: A phylogeny-based approach. *Medicinal Plants*, 1–48. <https://doi.org/10.1016/B978-0-08-100085-4.00001-3>
- Iftekhhar, S., Srivastava, V., & Sillanpaa, M. (2017). Enrichment of lanthanides in aqueous system by cellulose based silica nanocomposite. *Chemical Engineering Journal*, 320, 151–159. <https://doi.org/10.1016/j.cej.2017.03.051>
- Klavidià, L., & Spriòle, G. (2016). Optimisation of conditions for extraction of biologically active compounds from common bryophytes in Latvia. In Proceedings of the Latvian Academy of Sciences. Section B. *Natural, Exact, and Applied Sciences*, 69(6):299–306.
- Kumar, P., Pournara, A., Kim, K. H., Bansal, V., Rapti, S., & Manos, M. J. (2017). Metal-organic frameworks: Challenges and opportunities for ion-exchange/sorption applications. *Program in Material Science*, 86, 25–74. <https://doi.org/10.1016/j.pmatsci.2017.01.002>
- Lagergren, S. (1898). About the theory of so-called adsorption of soluble substances. *Kungl. Svenska vetenskapsakademiens handlingar*, 24(4), 1–39. <https://doi.org/10.1252/jcej.38.402>
- Martins, A. C., Pezoti, O., Cazetta, A. L., Bedin, K. C., Yamazaki, D. A., Bandoch, G. F., Asefa, T., Visentainer, J. V., & Almeida, V. C. (2015). Removal of tetracycline by NaOH-activated carbon produced from macadamia nut shells: Kinetic and equilibrium studies. *Chemical Engineering Journal*. <https://doi.org/10.1016/j.cej.2014.09.017>
- Meitei, M. D., & Prasad, M. N. V. (2013). Lead (II) and cadmium (II) biosorption on *Spirodela polyrhiza* (L.) Schleiden biomass. *Journal of Environmental Chemical Engineering*, 1(3), 200–207. <https://doi.org/10.1016/j.jece.2013.04.016>
- Mnif, A., Bejaoui, F., Mouelhi, M., & Hamrouni, B. (2017). Hexavalent chromium removal from model water and Cershock absorber factory effluent by nanofiltration and reverse osmosis membrane. *International Journal of Analytical Chemistry*, 3(1), 1–10. <https://doi.org/10.1155/2017/7415708>
- Mohammed, K., & Sahu, O. (2015). Bioadsorption and membrane technology for reduction and recovery of chromium from tannery industry wastewater. *Environmental Technology & Innovation*, 4, 150–158. <https://doi.org/10.1016/j.eti.2015.06.003>
- Naghypour, D., Taghavi, K., Ashournia, M., Jaafari, J., & ArjmandMovarrek, R. (2020). A study of Cr (VI) and NH_4^+ adsorption using greensand (glaucinite) as a low-cost adsorbent from aqueous solutions. *Water and Environment Journal*, 34(1), 45–56. <https://doi.org/10.1111/wej.12440>
- Naseem, K., Farooqi, Z. H., Begum, R., Ur Rehman, M. Z., Shahbaz, A., Farooq, U., Ali, M., Ur Rahman, H. M. A., Irfan, A., & Al-Sehemi, A. G. (2019). Removal of Cadmium (II) from aqueous medium using vigna radiata leave biomass: Equilibrium isotherms. *Kinetics and Thermodynamics, Zeitschrift fur Physikalische Chemie.*, 233, 669–690. <https://doi.org/10.1515/zpch-2018-1223>
- Norouzi, S., Heidari, M., Alipour, V., Rahmanian, O., Fazlzadeh, M., Mohammadi-Moghadam, F. ... & Dindarloo, K. (2018). Preparation, characterization and Cr (VI) adsorption evaluation of NaOH-activated carbon produced from Date Press Cake; an agro-industrial waste. *Bioresource Technology*, 258, 48–56. <https://doi.org/10.1016/j.biortech.2018.02.106>
- Nouha, K., Kumar, R. S., & Tyagi, R. D. (2016). Heavy metals removal from wastewater using extracellular polymeric substances produced by *Cloacibacterium normanense* in wastewater sludge supplemented with crude glycerol and study of extracellular polymeric substances extraction by different methods. *Bioresource Technology*, 212, 120–129. <https://doi.org/10.1016/j.biortech.2016.04.021>

- Nourmoradi, H., Avazpour, M., Ghasemian, N., Heidari, M., Moradnejadi, K., Khodarahmi, F., Javaheri, M., & Moghadam, F. M. (2016). Surfactant modified montmorillonite as a low cost adsorbent for 4-chlorophenol: Equilibrium, kinetic and thermodynamic study. *Journal of the Taiwan Institute of Chemical Engineers*, 59, 244–251. <https://doi.org/10.1016/j.jtice.2015.07.030>
- Panda, H., Tiadi, N., Mohanty, M., Mohanty, C.R. (2017). Studies on adsorption behavior of an industrial waste for removal of chromium from aqueous solution. *South African Journal of Chemical Engineering*, 23(1):132–138. <https://hdl.handle.net/10520/EJC-846a48efe>
- Pant, B. D., Neupane, D., Paudel, D. R., Lohani, P. C., Gautam, S. K., Pokhrel, M. R., & Poudel, B. R. (2022). Efficient biosorption of hexavalent chromium from water by modified arecanut leaf sheath. *Heliyon*, 8(4). <https://doi.org/10.1016/j.heliyon.2022.e09283>
- Pavesi, T., & Moreira, J. C. (2020). Mechanisms and individuality in chromium toxicity in humans. *Journal of Applied Toxicology*, 40, 1183–1197. <https://doi.org/10.1002/jat.3965>
- Prabhu, S. G., Srinikethan, G., & Hegde, S. (2020). Pelletization of pristine *Pteris vittata* L. pinnae powder and its application as a biosorbent of Cd (II) and Cr (VI). *SN Applied Science*, 2(1), 1–9. <https://doi.org/10.1007/s42452-019-1906-1>
- Pradhan, D., Sukla, L. B., Mishra, B. B., & Devi, N. (2019). Biosorption for removal of hexavalent chromium using microalgae *Scenedesmus* sp. *Journal of Cleaner Production*, 209, 617–629. <https://doi.org/10.1016/j.jclepro.2018.10.288>
- Qiu, B., Tao, X., Wang, H., Li, W., Ding, X., & Chu, H. (2021). Biochar as a low-cost adsorbent for aqueous heavy metal removal: A review. *J Analytical and Applied Pyrolysis*, 155, 105081. <https://doi.org/10.1016/j.jaap.2021.105081>
- Rahmani, A. R., Hossieni, E., & Poomohammadi, A. (2015). Removal of chromium (VI) from aqueous solution using electro-Fenton process. *Environmental Processes*, 2(2), 419–428. <https://doi.org/10.1007/s40710-015-0068-4>
- Saleh, T. A., Sari, A., & Tuzen, M. (2017). Optimization of parameters with experimental design for the adsorption of mercury using polyethylenimine modified-activated carbon. *Journal Environmental Chemical Engineering*, 5, 1079–1088. <https://doi.org/10.1016/j.jece.2017.01.032>
- Shahid, M., Shamsad, S., Rafiq, M., Khalid, S., Bibi, I., Niazi, N., Dumat, C., & Rashid, M. (2017). Chromium speciation, bioavailability, uptake, toxicity and detoxification in soil-plant system: A review. *Chemosphere*, 178, 513–533. <https://doi.org/10.1016/j.chemosphere.2017.03.074>
- Sharma, P., Hussain, N., Borah, D. J., & Das, M. R. (2013). Kinetics and adsorption behavior of the methyl blue at the graphene oxide/reduced graphene oxide nanosheet-water interface: A comparative study. *Journal Chemical Engineering Data*, 58(12), 3477–3488. <https://doi.org/10.1021/je400743r>
- Solisio, C., Lodi, A., & Finocchio, E. (2013). Effects of pH on chromate (VI) adsorption by *Spirulina platensis* biomass: Batch tests and FT-IR studies. *Water Science and Technology*, 67(9), 1916–1922. <https://doi.org/10.2166/wst.2013.070>
- Srivastava, S., Agrawal, S. B., & Mondal, M. K. (2016). Characterization, isotherm and kinetic study of Phaseolus vulgaris husk as an innovative adsorbent for Cr (VI) removal. *Korean Journal Chemical Engineering*, 33(2), 567–575. <https://doi.org/10.1007/s11814-015-0165-0>
- Teshale, F., Karthikeyan, R., & Sahu, O. (2020). Synthesized bioadsorbent from fish scale for chromium (III) removal. *Micron*, 130, 102817. <https://doi.org/10.1016/j.micron.2019.102817>
- Ume, O. L., Ekeoma, B. C., Yusuf, M., Al-Kahtani, A. A., Ubaidullah, M., & Sillanpää, M. (2022). Batch studies of hexavalent chromium biosorption from mining wastewater using *Aspergillus niger*. *Results in Chemistry*, 4, 100490. <https://doi.org/10.1016/j.rechem.2022.100490>
- Usman, A. R., Abduljabbar, A., Vithanage, M., Ok, Y. S., Ahmad, M., Ahmad, M., & Al-Wabel, M. I. (2015). Biochar production from date palm waste: Charring temperature induced changes in composition and surface chemistry. *Journal of Analytical and Applied Pyrolysis*, 115, 392–400. <https://doi.org/10.1016/j.jaap.2015.08.016>
- Weber, W. J., Jr., & Morris, J. C. (1963). Kinetics of adsorption on carbon from solution. *Journal of the Sanitary Engineering Division*, 89(2), 31–59.
- Xiong, H., Han, L., Zhang, H., Song, K., & Yang, Z. (2023). (2023) Approach for 3D in-situ visualizing the Cu (II) adsorption in corn cob biochar. *Water Air Soil Pollution*, 234, 2. <https://doi.org/10.1007/s11270-022-06014-9>
- Yusuff, A. S. (2019). Optimization of adsorption of Cr (VI) from aqueous solution by adsorbent prepared from *Leucaena leucocephala* seed shell using design of experiment. *Separation Science and Technology*, 54(15), 2418–2430. <https://doi.org/10.1080/01496395.2018.1547316>
- Zheng, C., Zheng, H., Wang, Y., Wang, Y., Qu, W., An, Q., & Liu, Y. (2018). Synthesis of novel modified magnetic chitosan particles and their adsorption performance toward Cr (VI). *Bioresource Technology*, 267, 1–8. <https://doi.org/10.1016/j.biortech.2018.06.113>
- Zouboulis, A. I., Kydros, K. A., & Matis, K. A. (1995). Removal of hexavalent chromium anions from solutions by pyrite fines. *Water Research*, 29(1995), 1755–1760. [https://doi.org/10.1016/0043-1354\(94\)00319-3](https://doi.org/10.1016/0043-1354(94)00319-3)

Publisher's Note Springer Nature remains neutral with regard to jurisdictional claims in published maps and institutional affiliations.

Springer Nature or its licensor (e.g. a society or other partner) holds exclusive rights to this article under a publishing agreement with the author(s) or other rightsholder(s); author self-archiving of the accepted manuscript version of this article is solely governed by the terms of such publishing agreement and applicable law.